

(C=C, C=N), 1435 s (P-C), 1098 (C-O), 746, 694 s cm⁻¹. Anal. Calcd for C₂₆H₂₃NCIOPPd: C, 58.01; H, 4.31; N, 2.60. Found: C, 58.06; H, 4.57; N, 2.55.

Acknowledgment. We acknowledge the financial support by the National Science Foundation (CHE 80-15354) and Dow Chemical, as well as the Englehard Cor-

poration for the loan of precious metals.

Supplementary Material Available: Listings of bond distances and angles, H atom coordinates, and thermal parameters (4 pages); a listing of observed and calculated structure factors (17 pages). Ordering information is given on any current masthead page.

Kinetic Deuterium Isotope Effects on Ligand Migrations in Metal Hydrides. 2¹

Julia Bracker-Novak, Sharad Hajela, Michael Lord, Minsheng Zhang, and Edward Rosenberg*

Department of Chemistry, California State University, Northridge, California 91330

Roberto Gobetto, Luciano Milone,* and Domenico Osella

Dipartimento di Chimica Inorganica, Chimica Fisica e Chimica dei Materiali, Università di Torino, Via Giuria 7-9, I 10125 Torino, Italy

Received July 6, 1989

Variable-temperature (VT) ¹H and ¹³C NMR studies of the complexes (μ-X)₂Os₃(CO)₉(μ₃-η²-(CH₃CH₂)₂C₂) (X = H or D) reveal that alkyne migration over the face of the cluster is directly linked to hydride migrations on the metal core as evidenced by a temperature-independent isotope effect (*k*_{HH}/*k*_{DD} = 1.7). In a related study of the VT ¹³C NMR of (μ-X)₂M₃(CO)₉(μ₃-S) (X = H or D; M = Ru, Os) the observation of a *k*_{HH}/*k*_{DD} = 1.6 for both the osmium and ruthenium complexes demonstrates that the first stage of carbonyl averaging is brought about by hydride migration and not axial-radial exchange of carbonyl groups, a process that occurs only at higher temperatures. The mechanistic implications of these results are discussed in the context of the reactivity of metal clusters and the dynamic properties of the metal-hydrogen bond.

Introduction

In our recent report on the kinetic deuterium isotope effects in ligand migrations we found *k*_{HH}/*k*_{DD} = 1.8 for the direct exchange of two hydride ligands in dihydride clusters and *k*_{HH}/*k*_{DD} = 1.5 for axial-radial exchange of carbonyl groups at the hydride bridged edge of the complexes H(μ-H)Os₃(CO)₁₀L.¹ Later, we used these results to interpret the observed kinetic deuterium isotope effects (*k*_{HH}/*k*_{DD} = 1.7) in the product distributions in the reaction of H₂O₃(CO)₁₀ with *tert*-butylacetylene.² We proposed that opening of the hydride bridge controlled edge-to-face (i.e., radial-to-axial) alkyne migration in the intermediate alkyne complex H(μ-H)Os₃(CO)₁₀(alkyne) and thereby controlled the observed product distributions. At about the same time Shore et al. noted an isotope effect (*k*_H/*k*_D = 1.5) in the bimolecular term of the rate law for the reaction of carbon monoxide with (μ-H)M₃(CO)₁₁⁻ (M = Ru, Os) which he also attributed to a rate-controlling opening of the hydride bridge to create a vacant site for coordination of the incoming carbonyl groups.³ It appears from these results that an understanding of factors controlling ligand migrations in metal clusters is extremely important in understanding their low-temperature reaction chemistry.

Our first observation of a kinetic deuterium isotope effect in metal cluster chemistry came as a result of our investigation of the two-step protonation of (μ-H)Ru₃-

(CO)₉(μ₃-η²-C₂^tBu) with protic acids.⁴ We found that the kinetic ratios of the two products formed depended upon whether deuterium was present in the starting cluster hydride or in the acid used. We rationalized these observations by invoking a mechanism where hydride migration was directly coupled to alkyne reorientation over the face of the cluster. Depending on the initial location of deuterium on the cluster one of the two possible hydride migrations would be faster, thus favoring the formation of one of the two kinetic products observed. However, at that time we had not established the connectivity between alkyne migration over the face of a trinuclear cluster and edge-to-edge migration of a hydride. In light of our previous results that established the connectivity between axial-radial carbonyl exchange and hydride bridge opening,¹ we thought it would be useful to extend these studies to the case of alkyne migration in a nonreactive system. We report here a VT ¹³C and ¹H NMR investigation of the complexes (μ-X)₂Os₃(CO)₉(μ₃-η²-(CH₃CH₂)₂C₂)⁵ (X = H or D) that lends strong support to our previously proposed mechanism⁴ and extends the "cog and wheel" view of cluster ligand dynamics to μ₃-alkyne trinuclear cluster systems.

We also report here a VT ¹³C NMR investigation of the ligand dynamics in (μ-X)₂M₃(CO)₉(μ³-S) (X = H or D; M = Ru, Os) in which the observed kinetic isotope effect differentiates between possible dynamic processes in a system where hydride motion is a "hidden process."⁶

(1) Part 1: Rosenberg, E.; Anslyn, E. V.; Barner-Thorsen, C.; Aime, S.; Osella, D.; Gobetto, R.; Milone, L. *Organometallics* 1984, 3, 1790.

(2) Rosenberg, E.; Anslyn, E. V.; Milone, L.; Aime, S.; Gobetto, R.; Osella, D. *Gazz. Chim. Ital.* 1988, 118, 299.

(3) Shore, S. G.; Leussing, D. L.; Payne, M. W. *J. Am. Chem. Soc.* 1987, 109, 617.

(4) Barner-Thorsen, C.; Rosenberg, E.; Saatjian, G.; Aime, S.; Milone, L.; Osella, D. *Inorg. Chem.* 1981, 20, 1592.

(5) Evans, J.; Johnson, B. F. G.; Lewis, J.; Matheson, T. W. *J. Organomet. Chem.* 1975, 97, C16.

(6) Forster, A.; Johnson, B. F. G.; Lewis, J.; Matheson, T. W. *J. Organomet. Chem.* 1976, 104, 225.

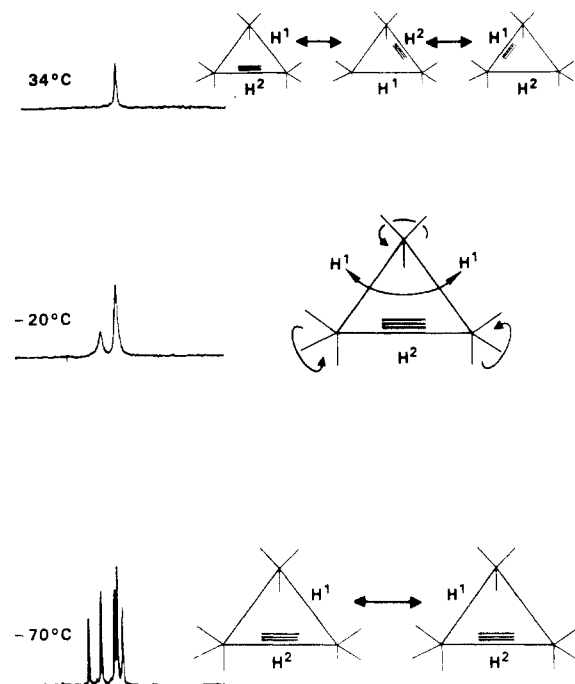
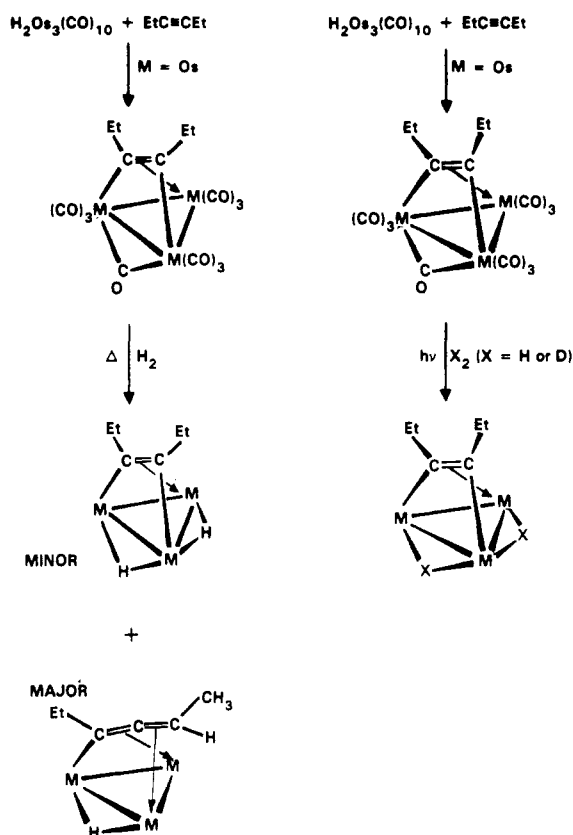


Figure 1. VT ^{13}C NMR of the carbonyl region of compound 1 at 20.1 MHz in $\text{CD}_3\text{C}_6\text{D}_5$ showing the three-stage exchange and the proposed ligand dynamics processes associated with each stage of the exchange (at the top of the figure not all possible hydrogen positions are illustrated for the sake of brevity).

Results and Discussion

VT ^1H and ^{13}C NMR Studies of $(\mu\text{-X})_2\text{Os}_3(\text{CO})_9(\mu_3\text{-}\eta^2\text{-(CH}_3\text{CH}_2)_2\text{C}_2)$. Complexes of the type $(\mu\text{-H})_2\text{Os}_3(\text{CO})_9(\mu_3\text{-}\eta^2\text{-R}_2\text{C}_2)$ ($\text{R} = \text{CH}_3, \text{H}$) have been previously examined by ^1H and ^{13}C NMR.⁵ It was concluded from the ^{13}C NMR data that there was a three-stage exchange process operative in these systems. The first stage of the exchange involved simple edge hopping of one hydride ligand which introduces a symmetry plane into the molecule (Figure 1), collapsing the low-temperature-limiting nine-line ^{13}C NMR spectrum to a five-line spectrum. The second stage of the exchange collapses the five-line carbonyl spectrum to a two-line spectrum in a 1:2 relative intensity and was thought to involve localized scrambling of carbonyl groups at each osmium center. The third stage of the exchange, which approximately overlaps with the onset of exchange between the two magnetically inequivalent hydrides, averages all of the carbonyl groups. It was unclear from that work whether alkyne motion or intermetallic scrambling (or both of these processes) was responsible for the averaging of all carbonyl environments in the last stage of the exchange. To check this point, we have examined the VT ^1H and ^{13}C NMR of the complex $(\mu\text{-H})_2\text{Os}_3(\text{CO})_9(\mu_3\text{-}\eta^2\text{-(CH}_3\text{CH}_2)_2\text{C}_2)$ (1), where motion of the alkyne can be tracked by following the dynamic behavior of the diastereotopic methylene protons on the alkyne. Recently, Deeming and co-workers have used a similar approach in delineating the relationship between alkyne motion and hydride exchange in the related complex $(\mu\text{-H})_2\text{Os}_3(\text{CO})_9(\mu_3\text{-}\eta^2\text{-HC}\equiv\text{COCH}_2\text{CH}_3)$.⁷ The preparation of 1 proved to be somewhat problematic. Unlike its dimethylacetylene analogue, thermal reaction of $(\mu\text{-CO})\text{Os}_3(\text{CO})_9(\mu_3\text{-}\eta^2\text{-(CH}_3\text{CH}_2)_2\text{C}_2)$ with H_2 at 80–100 °C does not give 1 as the major product but instead gives the C–H oxidative addition product $(\mu\text{-H})\text{Os}_3(\text{CO})_9(\mu_3\text{-}\eta^2\text{-}$

Scheme I



$\text{CH}_3\text{CH}_2\text{C}=\text{C}=\text{C}(\text{CH}_3)\text{H}$) as the major product and 1 as only a minor product (Scheme I). We have found that photolysis of $(\mu\text{-CO})\text{Os}_3(\text{CO})_9(\mu_3\text{-}\eta^2\text{-(CH}_3\text{CH}_2)_2\text{C}_2)$ with a medium-pressure mercury lamp under 1 atm of H_2 gave 1 as the only major product in moderate yield (Scheme I). It is interesting to note that $(\mu\text{-CO})\text{Os}_3(\text{CO})_9(\mu_3\text{-}\eta^2\text{-(CH}_3\text{CH}_2)_2\text{C}_2)$ apparently undergoes C–H oxidative addition much more slowly than the $\text{Os}_3(\text{CO})_{10}$ precursor to 1. We are currently examining the kinetics of this process and the photochemical reactivity of $(\mu\text{-CO})\text{Os}_3(\text{CO})_9(\mu_3\text{-}\eta^2\text{-alkyne})$ complexes in general.

The VT ^1H NMR of 1 shows a low-temperature-limiting ABX_3 pattern for the methylene protons at -20 °C. Above this temperature the methylene protons gradually merge and coalesce to give a quartet at $+50$ °C. Line-shape analysis in this temperature range gave a set of rate constants that were used to calculate a $\Delta H^\ddagger = 60 \pm 1$ kJ/mol for this process (Figure 2). Taken together with the ^{13}C NMR data (Figure 1) these experiments demonstrate that the alkyne in 1 undergoes an edge-to-edge migration over the cluster in the last stage of the carbonyl-exchange process. Line-shape analysis of the averaging of the two hydride resonances which takes place in the range -20 to $+50$ °C gave a slightly lower activation enthalpy of $\Delta H^\ddagger = 54 \pm 1$ kJ/mol. These results suggest but do not prove that hydride exchange and alkyne migration are coupled processes in 1.

To prove this last point, we synthesized a sample of $(\mu\text{-D})_2\text{Os}_3(\text{CO})_9(\mu_3\text{-}\eta^2\text{-(CH}_3\text{CH}_2)_2\text{C}_2)$ (1- d_2) according to Scheme I. The VT ^1H NMR of 1- d_2 was measured, and line-shape analysis gave a set of rate constants that gave $k_{\text{HH}}/k_{\text{DD}} = 1.6\text{--}1.7$ over the temperature range examined (Figure 2). The slight variation in the $k_{\text{HH}}/k_{\text{DD}}$ values at the different temperatures is within experimental error ($\approx 10\%$), and the observed isotope effects are thus temperature independent. These results clearly show that alkyne migration and hydride exchange are coupled pro-

(7) Deeming, A. J.; Boyar, E.; Felix, M. S. B.; Kabir, S. E. *J. Chem. Soc., Dalton Trans.* 1989, 5.

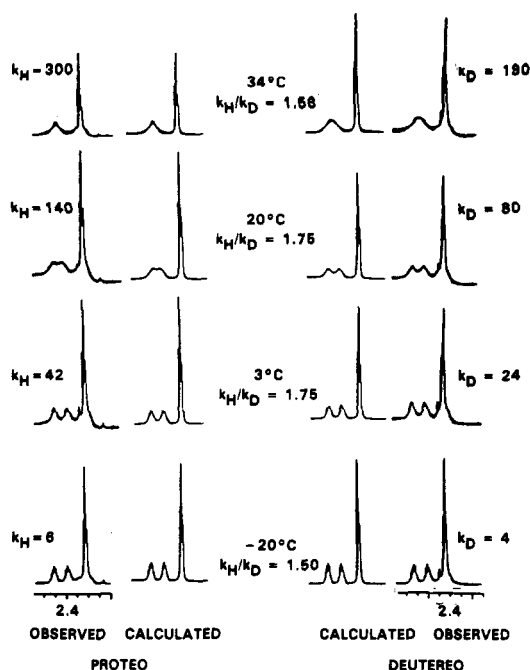


Figure 2. Calculated and observed VT ^1H NMR at 80 MHz of 1 and 1- d_2 in $\text{CD}_3\text{C}_6\text{D}_5$ showing the methyl and methylene protons.

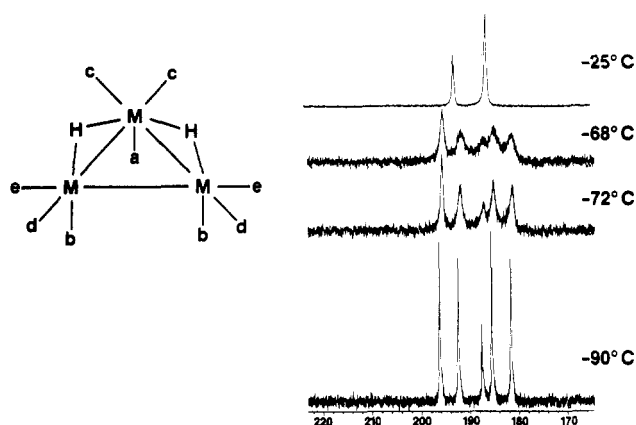


Figure 3. VT ^{13}C NMR of 3 in $\text{CD}_2\text{Cl}_2\text{-CFCl}_3$ showing the low-temperature-limiting spectrum and the first stage of exchange.

cesses in 1. They also lend further support to the mechanism proposed for the reaction of $\text{HRu}_3(\text{CO})_9(\mu_3\text{-}\eta^2\text{-C}_2\text{tBu})\text{P}(\text{C}_6\text{H}_5)_3$ with protic acids, where the coupled motion of an alkyne and one μ -hydride is required to give the observed product distribution.⁴ In fact the magnitude of $k_{\text{HH}}/k_{\text{DD}}$ for 1 is very similar to the observed changes in product distribution.

It should also be mentioned that we could visually observe a kinetic deuterium isotope effect on the low-temperature (-90 to -70 °C) hydride edge hopping of one hydride which averages the nine-line carbonyl spectrum to a five-line spectrum in 1- d_2 compared with 1. However, we could not perform line-shape analysis on this process due to accidental overlap of resonances in the intermediate exchange regime.

VT ^{13}C NMR Studies of $(\mu\text{-X}_2)\text{M}_3(\text{CO})_9\text{S}$ ($\text{M} = \text{Ru}$, Os ; $\text{X} = \text{H}$, D). The VT ^{13}C NMR spectra of the complexes $(\mu\text{-H})_2\text{M}_3(\text{CO})_9\text{S}$ ($\text{M} = \text{Ru}$ (2), Os (3)) were first reported by Johnson et al.⁶ A two-stage carbonyl-exchange process was observed. The low-temperature-limiting ^{13}C NMR spectra of 2 and 3 exhibit five carbonyl resonances in a ratio 1:2:2:2:2 consistent with the C_{2v} symmetry of these molecules in the solid state (Figure 3). As the temperature is increased, the carbonyl resonances in both

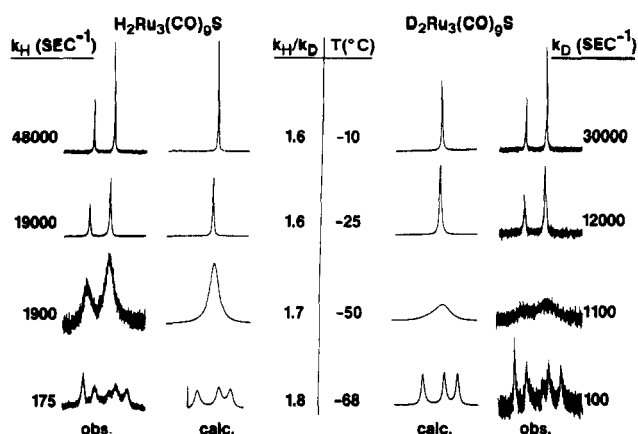
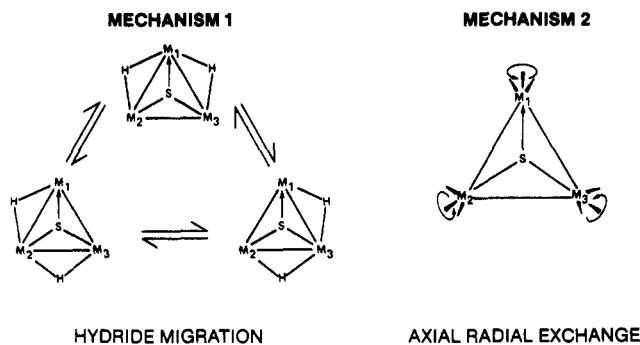


Figure 4. Calculated and observed VT ^{13}C NMR of 2 and 2- d_2 at 68 MHz in $\text{CD}_2\text{Cl}_2\text{-CFCl}_3$ in the carbonyl region.

Scheme II



2 and 3 collapse to two resonances in a 1:2 ratio. At higher temperatures these two resonances collapse to a single resonance. There are two possible explanations for these observations (Scheme II). Edge-to-edge migration of the hydrides could average all three equatorial carbonyl environments and both axial environments in the first stage of exchange, with the second stage of the exchange involving localized axial-radial exchange. Alternatively, the order of these two processes could be reversed with hydrides being static in the first stage of exchange and even in the second one if intermetallic scrambling of carbonyl groups is occurring.⁶ Later work made use of H-C couplings to make reasonable assignments of the carbonyl groups and indicated that hydride motion was indeed the low-energy process in 2.⁸ In light of our previous results¹ for the complex $(\mu\text{-H})\text{Ru}_3(\text{CO})_9(\mu_3\text{-}\eta^2\text{-C}_2\text{tBu})$ where we showed that axial-radial exchange of carbonyl groups at the hydride bridged ruthenium atoms was significantly slower than at the unbridged ruthenium atom and that hydride motion was the rate-determining step for axial radial exchange at the hydride-bridged edge ($k_{\text{HH}}/k_{\text{DD}} \approx 2$), we thought that a ^{13}C NMR investigation of $(\mu\text{-D})_2\text{M}_3(\text{CO})_9\text{S}$ ($\text{M} = \text{Ru}$ (2- d_2), Os (3- d_2)) would further elucidate the dynamic processes in 2 and 3.

The complexes 2- d_2 and 3- d_2 were prepared by exchange with excess trifluoroacetic acid followed by quenching in D_2O and recrystallization. Comparisons of the VT ^{13}C NMR spectra of 2 with 2- d_2 and 3 with 3- d_2 are shown in Figures 4 and 5, respectively. Line-shape analysis on the set of three resonances of relative intensity 2, which average with each other, gave a set of rate constants from which an average $k_{\text{HH}}/k_{\text{DD}} = 1.7$ was calculated for both 2 compared with 2- d_2 and 3 compared with 3- d_2 . These

(8) Aime, S.; Milone, L. *Prog. NMR Spectrosc.* 1977, 11, 183.

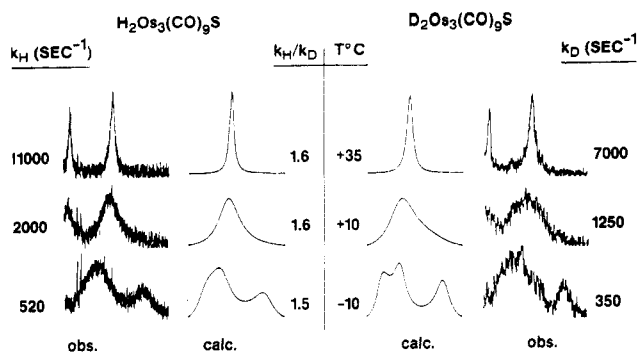


Figure 5. Calculated and observed VT ^{13}C NMR of **3** and **3-d₂** at 68 MHz in $\text{CD}_2\text{Cl}_2\text{-CFCl}_3$ in the carbonyl region.

results indicate hydride motion without axial-radial exchange is the first stage of exchange for **2** and **3**. No detectable isotope effect was observed for the second stage of the exchange for either **2-d₂** or **3-d₂** as would be expected since the hydrides are already in rapid motion in the temperature range where axial-radial exchange begins. These results closely resemble those obtained in a related dihydride system $[(\mu\text{-H})_2\text{Ru}_3(\text{CO})_9(\mu_3\text{-}\eta^2\text{-HC}\equiv\text{C}^t\text{Bu})]^{2+}$ where averaging of nonequivalent hydrides takes place at lower energies than axial-radial exchange of carbonyl groups.¹ The results obtained here for **2** and **3** do not clearly distinguish between simple sequential motion of one of the two hydrides in **2** or **3** and simultaneous motion of both hydrides. However the size of the isotope effect and the results obtained for **1** suggest that only sequential motion occurs in the first stage of exchange.

As would be expected from the reduced mass ($\mu = m_{\text{V}}m_{\text{H}}/(m_{\text{M}} + m_{\text{H}}) \cong 1$), the isotope effects observed here are about the same for osmium and ruthenium.⁹ The slightly larger activation enthalpy observed for **3** ($\Delta H^\ddagger = 51.0 \pm 1$ kJ) compared with **2** ($\Delta H^\ddagger = 43.5 \pm 1$ kJ) undoubtedly reflects the expected higher bond energy for the osmium-hydrogen bond compared with the ruthenium case.

Conclusions

The results reported here taken along with our prior results point to the fact that hydride ligand motion is involved in the rate-determining step of intramolecular migrations of alkyne ligands as well as carbonyl ligands and that the hydride ligand is among the most mobile ligands in valence-saturated polynuclear metal complexes. All of these processes exhibit a very narrow range of $k_{\text{H}}/k_{\text{D}}$ values (1.4–1.7).¹⁰ However, this may be accounted for by a heavy-atom effect (vide infra) since M–H vibrational levels are all relatively closely spaced. On the basis of zero-point energy differences, isotope effects for a linear symmetrical transition state involving a μ -hydride should be about 2, while those involving terminal hydrides should be about 3.5.^{9,10} Since there is no formal cleavage of the

M–H bonds in the ligand dynamics processes reported here, it is not surprising that the observed values are considerably smaller.

Experimental Section

Materials. $\text{Os}_3(\text{CO})_{12}$ and $\text{Ru}_3(\text{CO})_{12}$ were purchased from Stream Chemicals or synthesized from OsO_4 ¹¹ and $\text{RuCl}_3 \cdot 3\text{H}_2\text{O}$,¹² respectively, by known literature procedures. The complexes $(\mu_3\text{-}\eta^2\text{-}(\text{CH}_3\text{CH}_2)_2\text{C}_2)\text{Os}_3(\text{CO})_{10}$ ¹³ and $(\mu\text{-H})_2(\mu_3\text{-S})\text{M}_3(\text{CO})_9$ ($\text{M} = \text{Ru}, \text{Os}$)⁶ were synthesized by known literature procedures. The deuterated complexes $(\mu\text{-D})_2(\mu_3\text{-S})\text{M}_3(\text{CO})_9$ ($\text{M} = \text{Ru}, \text{Os}$) were prepared by exchange with excess $\text{CF}_3\text{CO}_2\text{D}$ followed by quenching with D_2O , extraction with CDCl_3 , and recrystallization from heptane to give >95% deuteration (by ^1H NMR). All solvents were stored over molecular sieves (Linde 4A).

Spectra. ^1H and ^{13}C NMR spectra were obtained on an IBM-NR80 or a JEOL-GX270 FT-NMR spectrometer. Probe temperatures were calibrated for ^1H NMR spectra with a methanol sample (containing 10% CD_3OD for field-frequency lock) and for ^{13}C NMR spectra by direct measurement with a thermometer in a 10-mm tube containing a suitable solvent. Temperature measurements are accurate to ± 2 °C. Line-shape analysis was performed using the DNMR4 line-shape analysis program.¹⁴ Errors in the calculated rate constants were estimated by varying the rate constant around the best-fit value until an observable change in the simulated spectrum could be visually detected when compared with the observed spectrum. This error proved to be 10% or less in all cases.

Photochemical Preparation of $(\mu\text{-X})_2\text{Os}_3(\text{CO})_9(\mu_3\text{-}\eta^2\text{-}(\text{CH}_3\text{CH}_2)_2\text{C}_2)$ ($\text{X} = \text{H}, \text{D}$). $\text{Os}_3(\text{CO})_{10}(\text{C}_2(\text{CH}_2\text{CH}_3)_2)$ ¹³ (100 mg, 0.11 mmol) was dissolved in 150 mL of cyclohexane in a Pyrex photolysis assembly. The reaction solution was degassed and saturated with H_2 for 30 min and then irradiated with ultraviolet light from a Hanovia medium-pressure mercury lamp (140 W) while the hydrogen flow was continued at a rate of 4 bubbles/s (outlet oil bubbler flow rate). The reaction was followed by analytical TLC (silica gel–hexane eluent) until the starting material spot almost disappeared, which took about 15 min. The solution turned from yellow to pale lemon after the photolysis. The reaction mixture was evaporated under vacuum, and the residue taken up in CH_2Cl_2 and then purified by preparative TLC (silica gel–hexane eluent) to yield 40 mg (45%) of $(\mu\text{-H})_2\text{Os}_3(\text{CO})_9(\mu_3\text{-}\eta^2\text{-}(\text{CH}_3\text{CH}_2)_2\text{C}_2)$ as cream-white crystals after recrystallization from hexane of the fastest moving band. Minor amounts (<10%) of $(\mu\text{-H})\text{Os}_3(\text{CO})_9(\mu_3\text{-}\eta^2\text{-}\text{CH}_3\text{CH}_2\text{C}\equiv\text{C}\equiv\text{CCHCH}_3)$ ¹⁵ were also obtained and identified. Compound **1**: IR (cm^{-1}) 2103 (w), 2093 (w), 2062 (s), 2040 (s), 2030 (vs), 2002 (s), 1980 (s), 1956 (m), 1934 (w); ^1H NMR (–50 °C) δ 3.27 (m, 2 H), 2.32 (m, 2 H), 1.18 (t, 6 H), –17.61 (s, 1 H), –21.32 (s, 1 H).

The deuterium analogue was synthesized in the same way by using D_2 instead of H_2 . It has the same ^1H NMR spectrum but showed no signal in the hydride region. There was no observation of incorporation of deuterium into the organic ligand.

Acknowledgment. We gratefully acknowledge the National Science Foundation (CHE8711549) for support of this research and the NATO Science Program (R.G. 0705/87; E.R. and L.M.) and Consiglio Nazionale delle Ricerche (L.M.).

(11) Cotton, F. A. *Inorg. Synth.* **1972**, *13*, 92.

(12) Basolo, F. *Inorg. Synth.* **1976**, *16*, 47.

(13) Rosenberg, F.; Gobetto, R.; Bracker-Novak, J.; Gellert, R. W. *J. Organomet. Chem.* **1989**, *365*, 163.

(14) Kleier, D. A.; Binsch, G. *QCPE* **1970**, *11*, 165.

(15) Skinner, D. M.; Rosenberg, E.; Bracker-Novak, J.; Aime, S.; Osella, D.; Gobetto, R.; Milone, L. *Organometallics* **1988**, *7*, 856.

(9) Norton, J. R.; Sullivan, J. M.; Edidin, R. T. *J. Am. Chem. Soc.* **1987**, *109*, 3945.

(10) Rosenberg, E. *Polyhedron* **1989**, *4*, 383, and references therein.